ISSN: 1231-4005
e-ISSN: 2354-0133
DOI: 10.5604/01.3001.0012.4368

MULTI-PARAMETRIC AND MULTI-OBJECTIVE THERMODYNAMIC OPTIMIZATION OF A SPARK-IGNITION RANGE EXTENDER ICE

Rastislav Toman, Ivaylo Brankov

Czech Technical University in Prague
Faculty of Mechanical Engineering
Department of Automotive, Combustion Engine and Railway Engineering
Technická Street 4, 166 07 Prague 6, Czech Republic
tel.: +420 776 792887
e-mail: rastislav.toman@fs.cvut.cz, ivaylo.brankov@fs.cvut.cz

Abstract

The current legislation pushes for the increasing level of vehicle powertrain electrification. A series hybrid electric vehicle powertrain with a small Range Extender (REx) unit – comprised of an internal combustion engine and an electric generator – has the technical potential to overcome the main limitations of a pure battery electric vehicle: driving range, heating, and air-conditioning demands. A typical REx ICE operates only in one or few steady-states operating points, leading to different initial priorities for its design. These design priorities, compared to the conventional ICE, are mainly NVH, package, weight, and overall concept functional simplicity – hence the cost-effectiveness. The design approach of the OEMs is usually rather conservative: parting from an already-existing ICE or components and adapting it for the REx application. The fuel efficiency potential of a one-point operation of the REx ICE is therefore not fully exploited. This article presents a multi-parametric and multi-objective optimization study of a REx ICE. The studied ICE concept uses a well-known and proven technology with a favourable production and development costs: it is a two-cylinder, natural aspirated, port injected, four-stroke SI engine. The goal of our study is to find its thermodynamic optimum and fuel efficiency potential for different feasible brake power outputs. Our optimization tool-chain combines a parametric GT-Suite ICE simulation model and modeFRONTIER optimization software with various optimization strategies, such as genetic algorithms, gradient based methods or various hybrid methods. The optimization results show a great fuel efficiency improvement potential by applying this multi-parametric and multi-objective method, converging to interesting short-stroke designs with Miller valve timings.

Keywords: *Range Extender, hybrid electric vehicle, battery electric vehicle, internal combustion engine, spark-ignition, thermodynamic optimization, genetic algorithm*

1. Introduction

The electric propulsion is desirable technology primarily for the vehicles used in urban areas with relatively short driving distances between the charging stops, because the pure battery electric vehicle (BEV) does not produce local tailpipe emissions. However, despite the continuous development of the battery technology, the BEVs still do not attain the customer acceptance of the conventional vehicles due to their limited driving range, long charging times, heating and air-conditioning problems, and high overall weight and cost, even for the mentioned urban applications with limited daily drive.

The Range Extender hybrid electric vehicle (HEV) powertrain could at the same time help achieves the desired customer acceptance and maintain the vehicle manufacturing cost. The Range Extender HEV operates usually as a pure electric vehicle, with the REx unit recharging the battery when necessary and extending the practical vehicle driving range. The REx unit is comprised of two main components: the electrical generator and typically an ICE. The key requirements for the REx ICE that usually operates in single-point steady state operation are low cost, NVH characteristic, package size and weight, and reasonable fuel efficiency [3].

Different automotive and engineering companies – such as AVL, MAHLE, KSPG, Lotus Engineering, and others – have presented their design studies on full REx units, sole REx ICEs or

REx HEV operation within the last 10 years. AVL reviewed a cost-oriented ICE design with an inline two-cylinder (R2) four-stroke SI engine with balancer shaft and power output of 18 kW [2]. Similar R2 engine was developed by MAHLE with a focus on the efficiency and intake noise optimization [8]. Subsequent study [3] presents some results from the engine testing, vehicle fuel consumption evaluation in different drive cycles, and C-segment vehicle package study. REx unit from KSPG and FEV combines a V2 90º ICE solution with two PMSM generators. The generators are coupled to the ICE crankshaft via so-called “Full Engine Vibration” compensator gear drive, enhancing the NVH behaviour [10]. Lotus Engineering published a very complex simulation and design study in 2010 [11]. The authors compared R2 and R3 engine configurations with an ICE power requirement of 38 kW using a parametrical study with an in-house engine simulation software. And finally, a more recent study from Tata Motors Europe and Bath University presents a development of a REx ICE from a production R2 engine for Indian market, optimizing intake and exhaust manifolds, and tuning the ECU [1].

Table 1 summarizes the main information on different REx ICE concepts: four from five engines are two-cylinders with a conservative square design (only Lotus RE35 is an R3 and long-stroke) and compression ratios of 10:1 to 11:1; the brake power outputs range from 18 to 37 kW at nominal engine speeds from 3500 RPM to 5000 RPM; and fuel consumptions of 240-250 g/kWh. All the presented engines are natural aspirated, four-strokes with port fuel injection system and stoichiometric operation.

Tab. 1. Concept comparison for different REx ICE solutions

REx Engine concept		AVL	MAHLE	TATA	Lotus	KSPG
Engine configuration		R2	R2	R2	R3	V2 (90º)
Valvetrain layout		SOHC	SOHC	SOHC	SOHC	OHV
Valves per cylinder	[–]	2	2	2	2	2
Engine displacement V_d	[dm^3]	0.570	0.900	0.624	1.193	0.799
Bore B	[mm]	70.0	83.0	73.5	75.0	80.0
Stroke S	[mm]	74.0	83.0	73.5	90.0	79.5
Bore/Stroke ratio $R_{B/S}$	[–]	0.946	1.000	1.000	0.833	1.006
Compression ratio r_c	[–]	11:1	10:1	10.3:1	10:1	N/A
Engine speed n_{ICE}	[RPM]	5000	4000	N/A	3500	4500
Mean piston speed c_s	[m/s]	12.333	11.065	N/A	10.500	11.925
Brake Power P_e	[kW]	18	30	~25	37	30
BSFC	[g/kWh]	~250	250	N/A	241	N/A

1.1. Article main goals

Development of the abovementioned research engines was mainly focused on the aspects of NVH or design simplicity to minimize production costs. Fuel consumption was clearly not the main focus. Only the Lotus Engineering team with their parametric approach were also aiming on the fuel consumption minimization.

Nevertheless, our department at Czech Technical University has a broad experience with different parametric optimization studies of internal combustion engines. For example, 2014 study on downsizing limits of a CI engine, using both thermodynamic and design optimization [4] or 2017 study on thermodynamic potential of electrical turbocharging for a small SI engine [13].

Here presented article is in line with this former research. Its main goal is to estimate the thermodynamic limits for a small REx engine working in a single-point steady operation, by the means of simulation. Different power output levels are considered: from 10 kW to 45 kW. Simulated combustion engine is naturally aspirated, spark-ignition, four-stroke, two-cylinder with two intake and two exhaust valves, port fuel injection, and stoichiometric operation.

2. Combustion engine model

A simulation model of the REx combustion engine was built in *GT-Suite* 0D/1D simulation software, which enables the simulation of a whole engine thermodynamic cycle. The engine is a virtual one, not calibrated by any experimental data. Hence, we use *GT-Suite* sub-models with high predictive abilities, and adequate experience with similar projects.

2.1. Main engine geometry

The REx model is fully parametrized, with the main parameters being the cylinder bore *B*, mean piston speed c_S, and bore/stroke ratio $R_{B/S}$.

Valve design parameters are linked to the cylinder bore using empirical formulas from [6] for a four-valve pent roof combustion chamber:

– intake valve diameter $D_{v_{in}} = 0.36 \cdot B$; maximum intake valve lift $L_{v_{in}} = 0.3 \cdot D_{v_{in}}$,
– exhaust valve $D_{v_{ex}} = 0.3 \cdot B$; maximum exhaust valve lift $L_{v_{ex}} = 0.3 \cdot D_{v_{ex}}$.

$R_{B/S}$ ratio with a cylinder bore define the engine stroke *S*; mean piston speed with stroke define the ICE operating speed n_{ICE}; and finally, conrod length is defined through a ratio of conrod length to crank radius *R* (a constant value of $R = 4$ is used). The 1D intake and exhaust air paths are also fully parametric and sized accordingly to the cylinder head. Generic flow coefficients C_D of the intake and exhaust valves are depicted on Fig. 1. Intake air path contains also an air filter, throttle, and intake manifold volume. Exhaust path then contains a simplified model of a catalyst brick, to get a realistic exhaust backpressure.

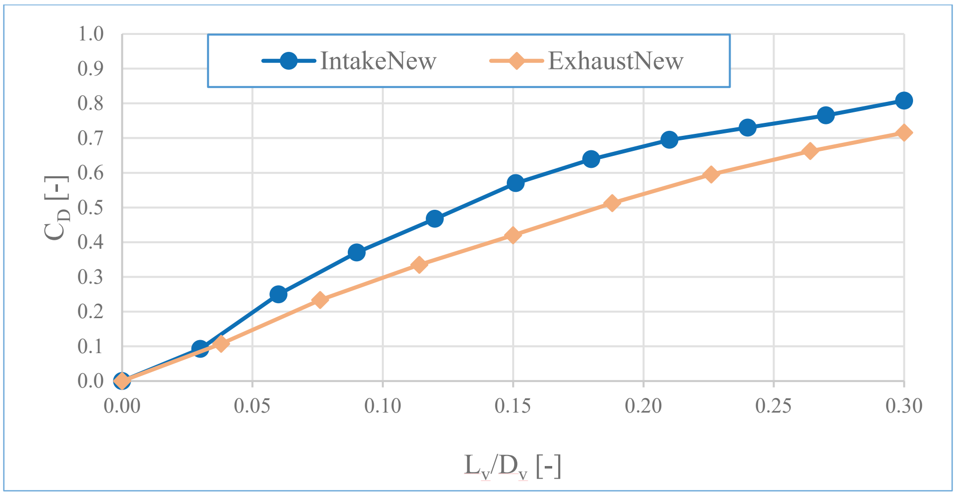

Fig. 1. Intake and exhaust valves flow coefficients

2.2. Heat transfer sub-model

In-cylinder heat transfer model used in this study is based on classical Woschni correlation without swirl [14]. Woschni formula estimates the heat transfer coefficient between the in-cylinder gas and cylinder walls. Structure and surface temperatures are obtained by a predictive finite element (FE) *GT-Suite* sub-model *EngCylTWallSoln*. FE model requires a simplified geometry of all the surfaces, together with coolant and oil boundary conditions. The cylinder structure geometry is also parametric and linked to the engine main geometry.

2.3. Engine friction sub-model

Another *GT-Suite* sub-model: *EngFrictionCF*, accounts for the mechanical efficiency or friction of the combustion engine. It is based on non-predictive Chen-Flynn model [7], with dependencies on engine speed and maximum in-cylinder pressure (equation 1):

$$FMEP = FMEP_{const} + A_{CF} \cdot p_{\max} + B_{CF} \cdot c_s + C_{CF} \cdot c_s^2 , \qquad (1)$$

where:
$FMEP_{const}$ – constant part of $FMEP$ = 0.4 bar,
A_{CF} – peak cylinder pressure factor = 0.005,
$p_{\max}$ – maximum in-cylinder pressure,
B_{CF} – mean piston speed factor = 0.09 bar/(m/s),
C_{CF} – mean piston speed squared factor = 0.0009 bar/(m/s)^2.

If the FMEP is known from the engine measurements, the Chen-Flynn formula can be calibrated. However, for our virtual engine, we have used the recommended values from [5].

2.4. Combustion and knock sub-models

Since the design of the combustion chamber is non-existent, an idealized SI combustion mode with knocking is applied.

A Vibe function [12] models the combustion process, but combustion phasing and duration are fully variable, regardless of the engine operating conditions or combustion chamber design and size. Therefore, the user – or in our case the automatic optimizer – can set any value for these two parameters in any condition. Fraction of fuel burned during combustion is set to a constant of 0.99.

The knock behaviour is then captured by the *Kinetic-Fit-Gasoline* knock model, based on the simulation of a detailed reaction kinetics. *Kinetic-Fit-Gasoline* uses three different induction times τ_i to capture the different chemistry of auto-ignition over a wide range of temperatures. A development of this model, together with some more details on the model formulas, is described in [15]. Fuel octane number necessary for the knock calculation is set to 95 for this study.

3. Optimization procedure

Our optimization tool-chain combines *GT-Suite* parametric ICE model and *modeFRONTIER* optimization software, applying a multi-strategy self-adapting algorithm *pilOPT*. *pilOPT* algorithm uses both a real and RSM-based (virtual) optimization in the search of the Pareto Frontier [9]. The optimization task is a multi-parametric and multi-objective one, with a goal of finding the thermodynamic optima for a defined engine P_e variant in a single-point operation.

There are 12 optimized parameters, namely: bore B, bore/stroke ratio $R_{B/S}$, mean piston speed c_s, compression ratio r_c, intake/exhaust valve timings (4 variables), intake/exhaust runner lengths (l_{in}, l_{ex}), combustion phasing CA50, and duration MFB10-90 (10-90% mass fraction burned).

The objective functions are always two: minimize the BSFC and a brake engine power P_e target for a. Engine P_e targets are varied from 10 kW to 45 kW with a step of 5 kW – 8 optimizations in total.

The optimizations are constrained by knocking and limited to the stoichiometric conditions. No other limits on maximum in-cylinder pressure or temperature were set.

4. Results

The optimization determined 8 different optimal sets for different engine P_e targets of a REx ICE that operates at single-point steady-state operation.

4.1. Optimal engine parameters

Table 2 contains first four optimized (independent – labelled with '*') parameters and three dependent. The optimization leads to short-stroke engines for each of the optimization variant, with $R_{B/S} \geq 1.5$ for each variant except the 10 kW.

Cylinder bore grows from 58.7 mm to 104.5 mm; engine displacement from 0.25 dm^3 to 1.16 dm^3.

The optimal mean piston speeds increase from 5.8 m/s for 10 kW variant to 7.55 m/s for 45 kW variant, leading to the engine speeds in a narrow range of 3350-3800 RPM.

The optimal compression ratio for all variants is exactly or very close to the parameter upper limit of 15:1.

Tab. 2. Optimal main engine parameters for different engine power targets

Optimization variant		10 kW	15 kW	20 kW	25 kW	30 kW	35 kW	40 kW	45 kW
B*	[mm]	58.70	70.10	78.40	84.70	90.40	95.50	100.00	104.50
$R_{B/S}$*	[–]	1.25	1.50	1.55	1.59	1.57	1.59	1.57	1.55
c_s*	[m/s]	5.80	5.90	6.20	6.50	6.95	7.05	7.40	7.55
r_c*	[–]	15.00	15.00	14.85	15.00	14.90	14.95	15.00	14.95
S	[mm]	46.96	46.73	50.58	53.27	57.58	60.06	63.69	67.42
V_d	[dm^3]	0.25	0.36	0.49	0.60	0.74	0.86	1.00	1.16
n_{ICE}	[RPM]	3705.28	3787.45	3677.30	3660.57	3621.07	3521.31	3485.40	3359.57

Table 3 summarizes four optimized valve-timing parameters: EVO, EVC, IVO, and IVC (all are reported at 1 mm valve lift; firing TDC represents a 0ºCA value) for all optimization variants. The optimal valve settings for all variants converged to the Miller cycle valve timing with EIVC (early intake valve close) and a small valve overlap period (Fig. 2).

Tab. 3. Optimal valve timing parameters for different engine power targets

Optimization variant		10 kW	15 kW	20 kW	25 kW	30 kW	35 kW	40 kW	45 kW
EVO	[ºCA]	152.10	150.33	149.27	143.73	141.29	141.89	143.31	146.50
EVC	[ºCA]	349.94	345.64	349.65	365.74	372.83	368.29	356.44	352.88
IVO	[ºCA]	372.13	365.34	356.72	362.91	355.32	357.22	339.96	352.21
IVC	[ºCA]	543.00	540.17	542.83	544.03	563.73	544.27	534.79	545.73

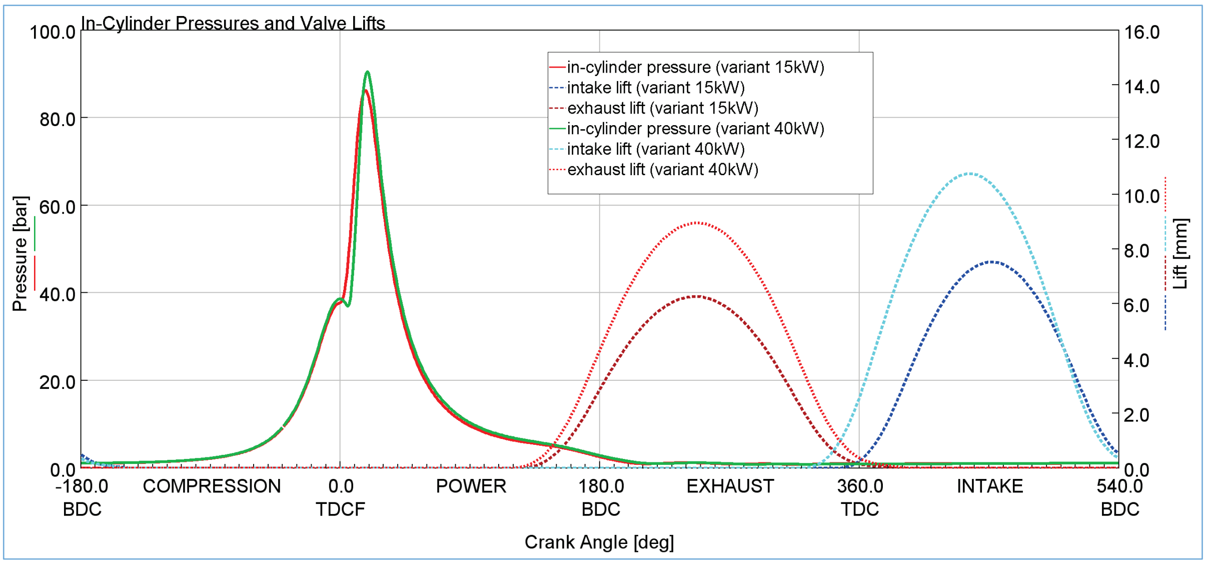

Fig. 2. In-cylinder pressures and valve lifts for 15 kW and 40 kW variants

Table 4 displays optimal parameters of the idealized SI combustion mode. The main combustion period shortens for higher engine P_e target variants and combustion phasing shifts slightly from the TDC to avoid knocking.

Tab. 4. Optimal combustion parameters for different engine power targets

Optimization variant		10 kW	15 kW	20 kW	25 kW	30 kW	35 kW	40 kW	45 kW
MFB10-90	[ºCA]	17.00	15.00	13.00	13.50	12.50	11.00	10.50	10.00
CA50	[ºCA]	12.50	12.50	12.50	13.00	12.50	14.00	13.00	15.00

And finally, Tab. 5 shows the optimal parameters of the intake and exhaust runner lengths. Additional sensitivity studies (not presented in this article) have shown us that the optimization is very sensitive to the main engine parameters (Tab. 2), valve timing (Tab. 3), and combustion phasing (Tab. 4 – CA50); and insensitive on combustion duration (Tab. 4 – MFB10-90) and intake/exhaust runner lengths (Tab. 5). Especially runner lengths from Tab. 5 are then more or less informative and not actual optima, suggesting only those shorter runners lead to lower pressure losses in the air paths.

Tab. 5. Optimal intake/exhaust runner lengths for different engine power targets

Optimization variant		10 kW	15 kW	20 kW	25 kW	30 kW	35 kW	40 kW	45 kW
l_{in}	[mm]	20.00	23.00	28.00	21.00	20.00	55.00	53.00	48.00
l_{ex}	[mm]	20.00	20.00	20.00	22.00	24.00	56.00	22.00	58.00

4.2. Engine output parameters

Table 6 presents the engine output parameters for 8 different P_e target variants. All variants with $P_e \geq 25$ kW achieve BSFC ~211 g/kWh (minima at 40 kW variant) indicating great theoretical BSFC potential. The lower P_e variants achieve BSFCs up to 3% worse than the optimal one (maxima at 10 kW variant). BMEP increases from the 12.83 bar of 10 kW variant to 13.90 bar of the 45 kW variant.

FMEP increases gradually from 10 kW variant to 45 kW variant, the same applies for the heat transfer loss (HTR loss). The important fact is that the values of FMEP and HTR loss seem realistic, although the respective sub-models must be further studied and refined.

The maximum in-cylinder pressures vary from 82.68 bar for 10 kW variant up to 93.74 bar of 40 kW variant. The maximum in-cylinder temperature of 2690 K is achieved by the 45 kW variant.

Tab. 6. Engine output parameters for different engine power targets

Optimization variant		10 kW	15 kW	20 kW	25 kW	30 kW	35 kW	40 kW	45 kW
BSFC	[g/kWh]	217.32	214.51	213.20	211.74	211.51	211.25	210.70	211.71
BMEP	[bar]	12.83	13.24	13.38	13.65	13.46	13.87	13.77	13.90
IMEP	[bar]	14.20	14.63	14.81	15.11	14.93	15.41	15.37	15.49
FMEP	[bar]	1.36	1.39	1.44	1.47	1.52	1.53	1.58	1.58
HTR loss	[kW]	6.07	8.35	10.44	12.10	13.98	15.50	17.61	18.65
$p_{\max}$	[bar]	82.28	86.26	88.83	88.37	89.40	90.48	93.74	89.49
$T_{\max}$	[K]	2548.23	2588.09	2629.36	2625.65	2650.44	2674.96	2690.39	2693.67

Table 7 then sums-up the efficiencies: indicated efficiency η_i, brake efficiency η_b, volumetric efficiency η_v, and mechanical efficiency η_m. Indicated efficiency achieves values greater than 40% for all variants; volumetric efficiency reaches very high values for a natural aspirated engine – for some variants slightly above 100%; and the mechanical efficiency values close to 90% that can be expected for this type of engine at full load operation.

Tab. 7. Engine efficiencies for different engine power targets

Optimization variant		10 kW	15 kW	20 kW	25 kW	30 kW	35 kW	40 kW	45 kW
η_i	[%]	41.93	42.43	42.78	43.07	43.33	43.29	43.61	43.32
η_b	[%]	37.90	38.39	38.63	38.89	38.93	38.99	39.11	38.90
η_v	[%]	96.29	98.11	98.54	99.78	98.01	101.34	100.32	101.78
η_m	[%]	90.37	90.51	90.35	90.35	90.12	90.02	89.56	89.73

5. Conclusions

The article deals with the multi-parametric and multi-objective thermodynamic optimization of a virtual naturally aspirated, spark-ignition, two-cylinder Range Extender SI combustion engine. The engine is optimized for a single-point steady-state operation and for different engine brake power output targets to find the full thermodynamic potential.

The main observations from the optimization are that the optimizer converges to the Miller valve timings and high compression ratio to increase the fuel efficiency. Then, large cylinder bore size leads to relatively large valve diameters also, compensating for the reduced intake duration by the EIVC. Mean piston speeds then balance the exact engine size with friction and heat transfer losses. These facts lead probably to the unconventional short-stroke configurations for this engine size and volumetric efficiencies around 100% even for a natural aspirated engine. The optimization algorithm also found an optimal combustion phasing to avoid knocking and still achieve great efficiencies, even for very high compression ratios.

The optimization results show qualitative trends and theoretical thermodynamic optima that can be used as a guideline for the REx ICE design. The best theoretical BSFC values are below 211 g/kWh. To further refine the optimization results, it is important to improve the engine friction, wall temperature FE, and combustion sub-models. SI combustion model used in this study is idealized. A refined combustion model should account for the cylinder bore size and ideally also for the in-cylinder turbulence to predict realistic combustion durations.

Our further work will focus on the optimizations of the single and three-cylinder natural aspirated and turbocharged engine versions. Friction and wall temperature FE sub-models will be improved using parametric CAD designs and in-house tools. And finally, the whole optimization process will be extended from sole thermodynamic optimization to both thermodynamic and design optimization.

Acknowledgements

This work was supported by the Grant Agency of the Czech Technical University in Prague, grant No. SGS16/213/OHK2/3T/12.

References

[1] Agarwal, A., Lewis, A., Akehurst, S., Brace, Ch., Gandhi, Y., Kirkpatrick, G., *Development of a low cost production automotive engine for range extender application for electric vehicles*, SAE Technical Paper, 2016-01-1055, 2016.

[2] Atzwanger, M., Hubmann, Ch., Schoeffmann, W., Kometter, B., Friedl, H., *Two-cylinder gasoline engine concept for highly integrated range extender and hybrid powertrain applications*, SAE Technical Paper, 2010-32-0130, 2010.

[3] Bassett, M., Hall, J., Oude Nijeweme, D., Darkes, D., Bisordi, A., Warth, M., *The development of a dedicated range extender engine*, SAE Technical Paper, 2012-01-1002, 2012.

[4] Bogomolov, S., Doleček, V., Macek, J., Mikulec, A., Vítek, O., *Combining thermodynamics and design optimization for finding ICE downsizing limits*, SAE Technical Paper, 2014-01-1098, 2014.

[5] *GT-POWER Engine Performance Application Manual*, Westmont: Gamma Technologies Inc., 2016.
[6] Heywood, J. B. *Internal combustion engine fundamentals*, McGraw-Hill, New York, 1988.
[7] Chen, S., Flynn, P., *Development of a single cylinder compression ignition research engine*. SAE Technical Paper 650733, 1965.
[8] Mahr, B., Bassett, M., Hall, J., Warth, M., *Development of an efficient and compact range extender engine*, MTZ, Vol. 72, No. 2011-10, pp. 738-746, 2011.
[9] *modeFRONTIER – Multi-Objective Design Environment*, version 4.4.3. [CD-ROM], 2012.
[10] Pischinger, M., Tomazic, D., Wittek, K., Esch, H.-J., Köhler, E., Baehr, M., *A low NVH range-extender application with small V-2 engine – based on a new vibration compensation system*, SAE Technical Paper, 2012-32-0081, 2012.
[11] Turner, J., Blake, D., Moore, J., Burke, P., Pearson, R., Patel, R., Blundell, D. Chandrashekar, R., Matteucci, L., Barker, P., Card, C., *The Lotus Range Extender Engine*, SAE Technical Paper, 2010-01-2208, 2010.
[12] Vibe, I. I., *Semi-empirical expression for combustion rate in engines*, In: Proc. Conference on Piston Engines, USSR Academy of Sciences, Moscow 1956.
[13] Vítek, O., Macek, J., *Thermodynamic potential of electrical turbocharging for the case of small passenger car ICE under steady operation*, SAE Technical Paper, 2017-01-0526, 2017.
[14] Woschni, G., *An universally applicable equation for the instantaneous heat transfer coefficient in the internal combustion engine*, SAE Technical Paper, 880198, 1967.
[15] Youngchul, R., Reitz, R. D., *A combustion model for IC engine combustion simulations with multi-component fuels*, Combustion and Flame, Vol. 158, No. 1, pp. 69-90, 2010.

Manuscript received 04 June 2018; approved for printing 07 September 2018